The images in Figure 2a and b demonstrate how balloon occlusion prevented dilution of the injected contrast material with nonopacified blood, improving visualization of the intraprostatic arteries. In addition, the images in Figure 2a and b demonstrate that an extraprostatic arterial anastomosis arising distal to the prostate that was visible on angiography with the balloon deflated was not visible after balloon inflation. This is thought to be due to greater flow of unopacified blood flowing through this anastomosis toward the catheter because the inflation of the balloon results in decreased arterial pressure at the catheter tip.

The changes in prostatic artery angiography with balloon occlusion point toward potential treatment advantages. Preventing nontarget embolization by avoiding particle reflux may not be the only mechanism. Improved visualization of intraprostatic arterial branches on angiography could help determine optimal catheter positioning and embolization endpoint. More importantly, the nonvisualization of extraprostatic anastomoses with balloon occlusion suggests the presence of a pressure gradient, drawing nonopacified blood toward the catheter tip. This phenomenon has been observed previously in both the liver and the spleen (3,4). For the purpose of PAE, this pressure gradient could be protective against inadvertent particle flow through distal collateral pathways resulting in nontarget embolization. As embolization of the prostate progresses, the pressure within the prostatic vessels would increase, eventually negating this effect.

There are also potential disadvantages of balloon occlusion PAE. First, the embolization endpoint is more difficult to discern, possibly leading to overembolization and nontarget embolization. Second, in traditional "free-flow" embolization, particles preferentially flow into hypervascular tissue, which is usually also the tissue being targeted. Occluding the systemic flow prevents preferential particle deposition in regions of higher vascularity, potentially resulting in a less complete embolization or even more nontarget embolization. Finally, if the balloon is overinflated, there is the potential for dissection of the targeted vessel, resulting in inability to treat.

In the cases described, balloon occlusion angiography demonstrated altered blood flow within and around the prostate compared with conventional angiography. Because a hand injection technique was used to produce these images, the changes described may not be as reproducible if a power injection were used. Also, contrast cone-beam computed tomography corresponding to the angiography was not performed, but it would have provided additional valuable information. Moving forward, data collection is needed to determine if the changes in blood flow observed with balloon occlusion angiography provide a treatment benefit.

REFERENCES

1. Kisilevzky N, Neto CL, Cividanes A. Ischemia of the glans penis following prostatic artery embolization. J Vasc Interv Radiol 2016; 27:1745–1747.
2. Uflacker A, Haskal ZJ, Bilhim T, Patrie J, Huber T, Pisco JM. Meta-analysis of prostatic artery embolization for benign prostatic hyperplasia. J Vasc Interv Radiol 2016; 27:1686–1697.
3. Irie T, Kuramochi M, Kamoshida T, Takahashi N. Selective balloon-occluded transarterial chemoembolization for patients with one or two hepatocellular carcinoma nodules: retrospective comparison with conventional super-selective TACE. Hepatol Res 2016; 46:209–214.
4. Rose SC, Lim GM, Arellano RS, Easter DB, Roberts AC. Temporary splenic artery balloon occlusion for protection of nonsplenic vascular beds during splenic embolization. AJR Am J Roentgenol 1998; 170:1186–1188.

Renal Microwave Ablation Resulting in Ureteropelvic Junction Stricture Remote from the Ablation Site

From: John J. Schmitz, MD
Grant D. Schmit, MD
Boyd R. Viers, MD
Thomas D. Atwell, MD
Departments of Radiology (J.J.S., G.D.S., T.D.A.) and Urology (B.R.V.)
Mayo Clinic
200 First Street SW
Rochester, MN 55902

Editor:

Percutaneous microwave (MW) ablation of renal masses has shown promising results (1). Although there are some potential benefits of MW ablation over radiofrequency ablation and cryoablation, the literature examining the potential complications of MW ablation is less robust compared with the literature for the aforementioned, more established renal ablation modalities (2,3). To highlight a potential serious complication related to percutaneous MW ablation in the kidney, 2 technically successful cases of percutaneous MW ablation of upper pole renal masses are presented that resulted in ureteropelvic junction (UPJ) strictures despite their remote locations. The need for institutional review board approval was waived as per institutional protocol.

Patient 1 was an 82-year-old man with a 2.5-cm renal mass and history of coronary artery disease, hypertension, and atrial fibrillation for which he was on long-term anticoagulation therapy. Patient 2 was an 87-year-old man with a 4.7-cm renal mass and a history of hypertension, atrial fibrillation, prostate cancer, and multiple nonmelanoma skin cancers. In both patients, biopsy proved the renal masses to be renal cell carcinoma, clear cell type. Both patients were managed with active surveillance by a urologist until they were ultimately referred for percutaneous thermal ablation secondary to interval growth.

The position of the tumors in both patients was such that transhepatic approaches were preferred, and MW ablation was chosen because of perceived potential for lower risk of bleeding complications compared with alternative

None of the authors have identified a conflict of interest.

Figure E1 is available online at www.jvir.org.

http://dx.doi.org/10.1016/j.jvir.2017.03.010

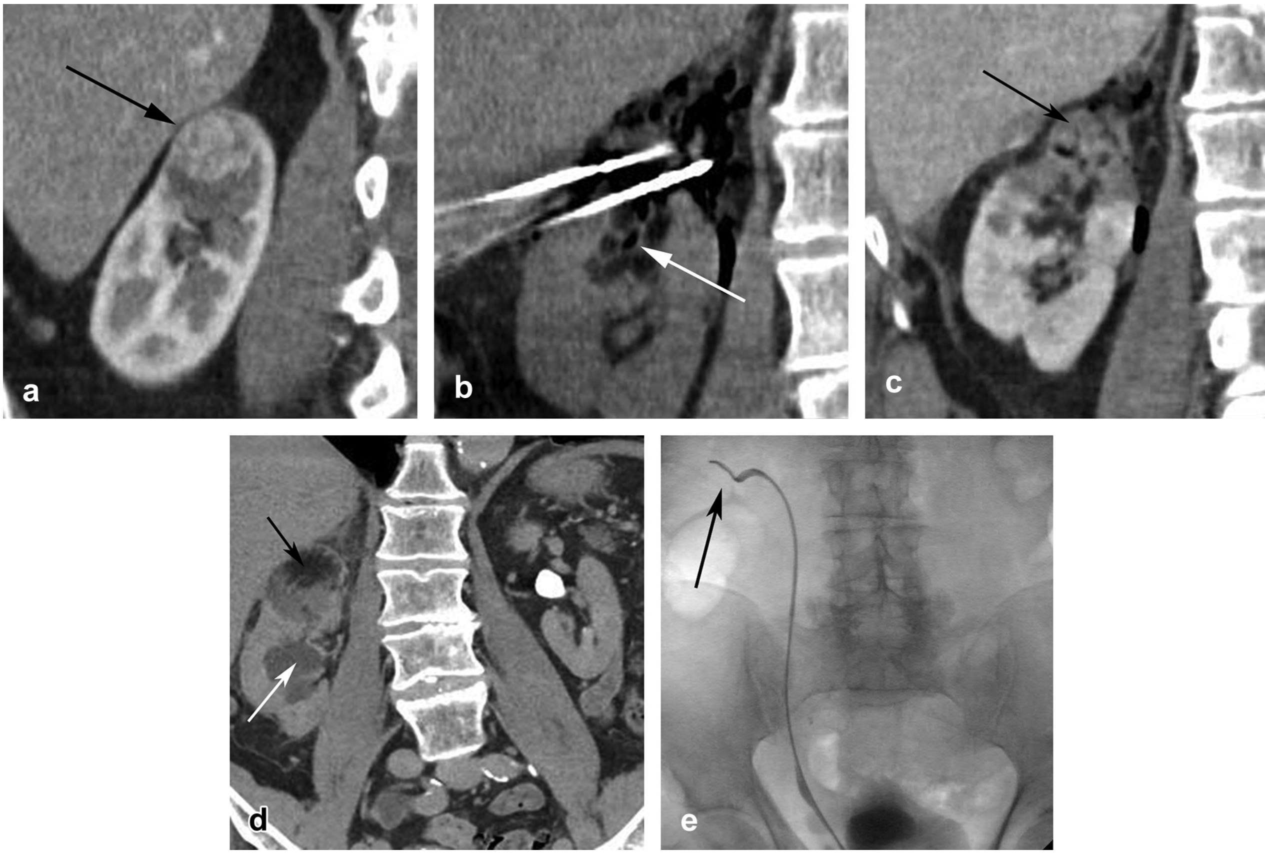

Figure. Patient 1 underwent ablation of a 2.5-cm mass in the upper right kidney. **(a)** Coronally reconstructed CT image with intravenous contrast enhancement shows the 2.5-cm mass in the upper right kidney (black arrow). **(b)** Coronally reconstructed CT image obtained during MW ablation shows the 3 antennas in the mass with adjacent soft tissue gas and gas within the collecting system (white arrow). **(c)** Coronally reconstructed CT image with intravenous contrast enhancement obtained immediately after ablation shows an ablation defect encompassing the index renal mass (black arrow) but not extending to the UPJ. **(d)** Delayed coronally reconstructed CT image with intravenous contrast enhancement obtained 3 months after ablation shows a large evolving ablation site (black arrow) with associated fat necrosis and new dilatation of the intrarenal collecting system (white arrow) and absence of contrast material excretion from the right kidney. **(e)** Fluoroscopic image obtained during retrograde pyelography with attempted ureteral stent placement. No contrast material could be refluxed into the right renal pelvis. A pinhole UPJ stricture was noted that a wire would not pass beyond (black arrow).

cryoablation for these relatively larger masses. Both patients were treated with percutaneous MW ablation under general anesthesia by board certified radiologists (patient 1 treated by J.J.S. with 5 y of experience and patient 2 treated by G.D.S. with 14 y of experience) and spent 1 night in the hospital after the ablation procedure. The technique was similar to the technique that has been described for renal mass cryoablation (3). Using ultrasound guidance, the MW antennas were placed into the targeted masses via a transhepatic approach, and satisfactory position was confirmed with computed tomography (CT).

Patient 1 was treated with 2 MW antennas for 10 minutes at 65 W (**Fig a–e**). In patient 1, neither of the 2 antennas violated the collecting system. Patient 2 was treated with 3 identical MW antennas for 10 minutes at 65 W followed by a 2-cm pullback and repeat ablation for 5 minutes at 65 W because of the larger size of the tumor (**Fig E1a–c** [available online at *www.jvir.org*]). In patient 2, an upper pole calyx was traversed by 1 of the 3 antennas. Both ablations were actively monitored with ultrasound and intermittent CT scanning.

After tumor ablation, the antennas were removed with cauterization of the tracts. No immediate complications were manifested by either patient. Follow-up CT scans at 3 months (patient 1) and 9 months (patient 2) demonstrated new right UPJ obstruction in both cases. In patient 1, attempts were made to place a retrograde ureteral stent once the obstruction was noted, but the stricture was too tight to pass even a wire. Both patients were asymptomatic through 18 months of follow-up. Estimated glomerular filtration rate in patient 1 (calculated using Modification of Diet in Renal Disease equation) was > 60 mL/min/1.73 m^2 before ablation and had stabilized at 51 mL/min/1.73 m^2 at the 18-month follow-up examination. Estimated glomerular filtration rate in patient 2 was > 60 mL/min/1.73 m^2 before ablation and at the 18-month follow-up examination, but his serum creatinine value increased from 0.7 mg/dL to 1.1 mg/dL.

These cases of UPJ stricture after MW ablation differ from previous reports in the literature, which primarily address radiofrequency ablation of tumors and local urothelial injury. Both of these cases demonstrate remote urothelial damage from MW ablation. The suspected